# Establishment and characterization of novel highly aggressive HER2-positive and triple-negative breast cancer cell lines

SUYANEE THONGCHOT[1,2], PRANISA JAMJUNTRA[1], JATURAWITT PRASOPSIRI[1], PETI THUWAJIT[1], NUNGHATHAI SAWASDEE[2], NARAVAT POUNGVARIN[3], MALEE WARNNISSORN[4], DOONYAPAT SA-NGUANRAKSA[5], PORNCHAI O-CHAROENRAT[6], PA-THAI YENCHITSOMANUS[2] and CHANITRA THUWAJIT[1]

[1]Department of Immunology, [2]Siriraj Center of Research Excellence for Cancer Immunotherapy (SiCORE-CIT), Research Department, and Departments of [3]Clinical Pathology, [4]Pathology, [5]Surgery, Faculty of Medicine Siriraj Hospital, Mahidol University, Bangkok 10700; [6]Breast Center, Medpark Hospital, Bangkok 10110, Thailand

Received July 27, 2021; Accepted September 16, 2021

DOI: 10.3892/or.2021.8205

**Abstract.** Breast cancer cell lines are widely used as an *in vitro* system with which to study the mechanisms underlying biological and chemotherapeutic resistance. In the present study, two novel breast cancer cell lines designated as PC-B-142CA and PC-B-148CA were successfully established from HER2-positive and triple-negative (TN) breast cancer tissues. The cell lines were characterized by cytokeratin (CK), α-smooth muscle actin (α-SMA), fibroblast-activation protein (FAP) and programmed death-ligand 1 (PD-L1). Cell proliferation was assessed using a colony formation assay, an MTS assay, 3-dimensional (3-D) spheroid and 3-D organoid models. Wound healing and Transwell migration assays were used to explore the cell migration capability. The responses to doxorubicin (DOX) and paclitaxel (PTX) were evaluated by 3-D spheroids. The results showed that the PC-B-142CA and PC-B-148CA cell lines were α-SMA-negative, FAP-negative, CK-positive and PD-L1-positive. Both cell lines were adherent with the ability of 3-D-multicellular spheroid and organoid formations; invadopodia were found in the spheroids/organoids of only PC-B-148CA. PC-B-142CA had a faster proliferative but lower metastatic rate compared to PC-B-148CA. Compared to MDA-MB-231, a commercial TN breast cancer cell line, PC-B-148CA had a similar $CD44^+/CD24^-$ stemness property (96.90%), whereas only 8.75% were found in PC-B-142CA. The mutations of *BRCA1/2*, *KIT*, *PIK3CA*, *SMAD4*, and *TP53* were found in PC-B-142CA cells related to the resistance of several drugs, whereas PC-B-148CA had mutated *BRCA2*, *NRAS* and *TP53*. In conclusion, PC-B-142CA can serve as a novel HER2-positive breast cancer cell line for drug resistance studies; while PC-B-148CA is a novel TN breast cancer cell line suitable for metastatic and stemness-related properties.

*Correspondence to:* Professor Chanitra Thuwajit, Department of Immunology, Faculty of Medicine Siriraj Hospital, Mahidol University, 2 Wang Lang Road, Bangkoknoi, Bangkok 10700, Thailand
E-mail: cthuwajit@yahoo.com

*Abbreviations:* α-SMA, α-smooth muscle actin; BRCA1/2, breast cancer 1/2; CK, cytokeratin; DOX, doxorubicin; ER, estrogen receptor; ERBB2, erb-b2 receptor tyrosine kinase 2; FAP, fibroblast-activation protein; HER2, human epidermal growth factor receptor 2; KIT, tyrosine-protein kinase; PD-L1, programmed death-ligand 1; PIK3CA, phosphatidylinositol-4,5-bisphosphate 3-kinase catalytic subunit α; PR, progesterone receptor; PTX, paclitaxel; SMAD4, mothers against decapentaplegic homolog 4; TP53, tumor protein p53

*Key words:* breast cancer, cell line, migration, cytotoxicity, mutation

## Introduction

In the female population, breast cancer exhibits the highest cancer incidence and is a leading cause of death worldwide (1,2). It was estimated in 2018 that more than 2.1 million women were newly diagnosed with breast cancer with 600,000 deaths (3) and 2.3 million new cases are estimated by 2030 (4). Although breast conservation surgery combined with neoadjuvant therapy can reduce the mortality rate, some breast cancer patients have potential drug-resistance genetic profiles leading to the unsatisfactory outcome of treatments (5).

Breast cancer is categorized into 4 major subtypes based on the presence or absence of molecular markers by immunohistochemical staining for the estrogen receptor (ER), progesterone receptor (PR) and human epidermal receptor 2 (HER2): luminal subtypes, A and B: ER-positive and/or PR-positive/HER2-negative (luminal A) or -positive (luminal B) accounted for 70% of breast cancer cases; HER2-positive subtype: ER- and/or PR-negative/HER2-positive with an estimation of 15-20%, and triple-negative (TN) or basal subtype: lacking all ER/PR/HER2 with around 15% of the total cases (6). Luminal and HER2-positive subtypes respond well to standard treatment; however, some of them have treatment failures (5). The TN subtype is of great interest to explore

since having no ER/PR/HER2, these patients with advanced stage have no targeted drugs available.

Several breast cancer cell lines have been widely used in research to unravel the mechanisms of cancer progression and drug resistance driven by certain genes (7). There are 27 TN breast cancer cell lines used in breast cancer research filed of which MDA-MB-231 is the most popular cell line with high proliferative, invasive, and metastatic properties (8). The trastuzumab-resistant HER2-positive MDA-MB-453 cell line has an abnormal gene expression profile, in particular, the upregulation of transforming growth factor (TGF)-β1 and epidermal growth factor (EGF), and insulin-liked growth factor binding protein-3 (IGFBP3) (9). Although, novel breast cancer cell lines have been established (10-12), no recent cell models of TN and HER2-positive subtypes have been reported for mechanistic investigation of metastasis and drug resistance.

In the present study, two novel breast cancer cell lines designated as PC-B-142CA and PC-B-148CA were established from fresh breast cancer tissues. The epithelial markers and chromosome aberrations were investigated to confirm epithelial-derived cancer cells. The 2-dimensional (2-D) and 3-D tumor spheroids and 3-D organoids were used to demonstrate the tumorigenic phenotypes including cell proliferation, cell growth, cell migration, cancer stemness (CSCs) and doxorubicin (DOX)/paclitaxel (PTX) resistance. The DNA sequences of drug-targeted genes were investigated and discussed for the chemotherapeutic and target drugs response of these cells. Programmed death-ligand 1 (PD-L1) was checked to propose its use for the sensitivity of cancer cells by T cell killing. The obtained findings revealed that PC-B-148CA is a good TN breast cancer model for investigating migration and cancer stemness properties, while PC-B-142CA is a new HER2-positive breast cancer model for drug resistance.

## Materials and methods

*Cancer cell isolation and culture*. Breast cancer tissues were obtained from two patients who underwent surgery at Siriraj Hospital, Bangkok, Thailand, designated as PC-B-142CA and PC-B-148CA. PC-B-142CA was derived from a 58-year-old female patient diagnosed with stage IV HER-2 positive breast cancer, while PC-B-148CA was isolated from a 50-year-old female patient diagnosed with stage II TN breast cancer.

The tissue collection protocol was approved by the Siriraj Institutional Review Board (COA no. Si 329/2017). Single cell suspensions from tumor tissues were prepared using the GentleMACS single cell isolation machine (Miltenyi Biotec GmbH) according to the manufacturer's instructions. Briefly, the tissues were minced into 1-2 $mm^3$ pieces and incubated for 30 min at 37˚C with the enzyme cocktail mix (Miltenyi Biotec GmbH). The digested cells were harvested and filtered over a 70 $\mu$m nylon filter (SPL Life Sciences). The cell suspensions were washed by centrifugation and the cell pellets were resuspended in DMEM F/12 media (Gibco BRL) supplemented with 10 ng/ml of epidermal growth factor (EGF, PeproTech, Inc.), 5 $\mu$g/ml insulin (Sigma-Aldrich; Merck KGaA), 0.32 $\mu$g/ml hydrocortisone (Sigma-Aldrich; Merck KGaA) and 10 $\mu$M ROCK inhibitor (Y27632, StemMACS, Miltenyi Biotec GmbH). The contaminated fibroblasts were isolated using a tumor cell isolation kit (Miltenyi Biotec GmbH). The primary breast cancer cells were cultured in DMEM F/12 medium supplemented with 10% fetal bovine serum (FBS) (Thermo Fisher Scientific Inc.) and 10X antibiotic mixture containing 1 U/ml penicillin G sodium and 1 mg/ml streptomycin (Thermo Fisher Scientific, Inc.). Cells were subcultured, periodically checked for negative mycoplasma and kept in liquid nitrogen for storage.

Commercial human breast cancer cell lines, MDA-MB-231 and MCF-7 (purchased from American Type Culture Collection, ATCC) were cultured at 37˚C in a humidified atmosphere of 5% $CO_2$ in Dulbecco's modified Eagle's medium (DMEM, Gibco, Thermo Fisher Scientific Inc.) supplemented with 10% FBS (v/v) (Gibco, Thermo Fisher Scientific Inc.), 100 U/ml of penicillin and 100 $\mu$g/ml of streptomycin (both from Sigma-Aldrich; Merck KGaA).

*Detection of epithelial markers by immunocytochemistry and immunofluorescence staining*. Cell pellets were fixed in 10% formalin and subjected for staining on sterile glass coverslips by antibodies against estrogen receptor (rabbit anti-ER monoclinal antibody, 790-4325, ready-to-use; clone SP1, Ventana Laboratories), progesterone receptor (rabbit anti-PR monoclonal antibody, 790-4296, ready-to-use; clone 1E2, Ventana Laboratories) and human epidermal growth factor receptor 2 (rabbit anti-HER2 monoclonal antibody, 790-2991, ready-to-use; clone 4B5, Ventana Laboratories). This process was performed by the routine service at the Department of Pathology, Faculty of Medicine, Siriraj Hospital, Mahidol University. Ki-67 (1:300 dilution, M7240, rabbit anti-Ki-67 monoclonal antibody, clone MIB-1, Dako Laboratories; Agilent Technologies, Inc.) percentages at cut-point <14% were defined as luminal A subtype (13,14).

The epithelial cytokeratin (CK) including CK-4, -5, -6, -8, -10, -13, -18 and -19 were investigated. α-SMA and FAP, specific markers for the stromal fibroblast, were used as a quality control of cancer cell purity. The presence of PD-L1 was evaluated for the ability of the obtained cancer cells to resist T cell killing. Cells at $1x10^4$ were plated on sterile glass coverslips for 24 h, fixed in ice-cold absolute methanol, permeabilized with 0.2% Triton-1X PBS, and then incubated overnight at 4˚C in a humidified chamber with the indicated primary antibody as follows: mouse anti-human panCK antibody (dilution 1:200, sc-8018, Santa Cruz Biotechnology, Inc.), mouse anti-human CK-19 antibody (dilution 1:200, sc-6278, Santa Cruz Biotechnology, Inc.), mouse anti-human α-SMA antibody (dilution 1:500, A5228, Sigma-Aldrich; Merck KGaA), rabbit anti-human fibroblast activation protein (FAP) antibody (dilution 1:500 ab53066, Abcam), and rabbit anti-human PD-L1 antibody (dilution 1:500, ab205921, Abcam). The goat anti-mouse IgG-Cy3 antibody (dilution 1:2,000, #115-166-071, Jackson ImmunoResearch Laboratories Inc.) or the donkey anti-rabbit IgG (H+L) highly cross-adsorbed secondary antibody, Alexa Fluor 488 (dilution 1:2,000, 21206, Thermo Fisher Scientific, Inc.) was applied for 3 h at room temperature. The nuclei were stained with 1:2,000 Hoechst 33342 (Invitrogen, Thermo Fisher Scientific, Inc.). Fluorescence was captured with a ZEISS LSM 800 confocal laser fluorescence scanning microscope (Axio Observer7, LSM 800, Zeiss GmbH).

*Three-dimensional (3-D) spheroid and 3-D organoid formation*. Spheroids were created by $1x10^3$ breast cancer cells supplemented with 2.5% cold Matrigel™ (BD Biosciences) in 200 $\mu$l of complete DMEM F/12 medium and seeded into individual wells of pre-cooled 96-well ultra-low attachment multiple well plates (CLS7007, Costar/Corning, Inc.). Centrifugation at 4˚C at 300 x g for 3 min was performed and the cells were maintained at 37˚C in a humidified 5% $CO_2$ atmosphere for 5 days to form spheroids. Medium was renewed twice weekly and the proliferation rate of spheroids was monitored for up to 10 days. For the organotypic cultures, $1x10^4$ of PC-B-142 and PC-B-148CA cells were generated in 24-well clear flat bottom ultra-low attachment multiple well plates (CLS3473, Costar/Corning, Inc.) at the concentration of 4% cold Matrigel™ (BD Biosciences) in 300 $\mu$l of complete DMEM F/12 medium. The plate was placed in the incubator with 5% $CO_2$ at 37˚C. The organoid culture medium was refreshed with 300 $\mu$l complete DMEM F/12 medium every 2-3 days. The organoid culture was ended on day 14.

*Cell proliferation and colony formation assays*. Growth curves of PC-B-142CA and PC-B-148CA cells, compared to commercial cell lines, MDA-MB-231 and MCF-7, were determined by using the MTS (3-(4,5-dimethylthiazol-2-yl)-5-(3-carboxymethoxyphenyl-2-(4-sulfophenyl)-2H-tetrazolium) (G3581, Promega.) assay following the manufacturer's instructions. Briefly, 5,000 cells were seeded in each well of 96-well plates in complete DMEM F/12 medium and cultured overnight in a 5% $CO_2$ atmosphere at 37˚C. At time intervals, 20 $\mu$l of MTS reagent was added to each well, followed by incubation in a humidified, 5% $CO_2$ atmosphere for a minimum of 2 h. Absorbance at 490 nm was recorded at 24, 48, 72 and 96 h. For the colony formation assay, 2,000 cancer cells were seeded in 6-well plates in complete DMEM F/12 medium and cultured overnight. The medium was refreshed every 3 days. At day 10, the adherent cells were washed with 1X PBS, fixed with cold methanol, and stained with a 0.5% crystal violet solution. The colony numbers were counted by photometric measurements using CellCounter software version 0.2.1 (Nghia, Ho) and a 1-5 $\mu$m diameter colony was determined as one colony. Three independent experiments were performed for each assay condition.

*Drug cytotoxicity assay*. The 2-D culture was treated for 0, 24, 48 and 72 h with 0, 0.01, 0.1, 1 and 10 $\mu$M DOX (Selleckchem) or PTX (Selleckchem) diluted in 10% FBS of DMEM/F12 medium. The selected concentrations at 0.1, 1 and 10 $\mu$M of DOX or PTX were tested in 3-D spheroids for 72 h. The 2-D killing was measured by the MTS assay and cell viability of 3-D killing was analyzed by the calculation of the volume ($\mu m^3$) with the formula $4/3\pi r^3$ in a spheroid with or without drug treatment.

*Cell migration assay*. For the wound healing assay, $5x10^4$ cells were adhered in a 24-well plate and cultured until they reached >90% confluency. Scratch wounds were made with a sterile yellow tip pipette. The cells were incubated in complete 10% FBS DMEM F/12 and the wound area was recorded and digitally photographed at 30 min, 18 and 24 h by an inverted microscope (IX71 Olympus). The closing of the wound gap was calculated using ImageJ software version 1.48v (NIH, Bethesda, MD, USA). Quantification of cell migration was determined with the formula: Migration area=(Area of original wound-Area of wound after healing)/Area of original wound. Cell migration was performed in 8.0-$\mu$m Transwell Boyden chambers (Corning, Inc.). A total of $5x10^4$ cells in serum-free medium were seeded in the upper chamber insert. Subsequently, 500 $\mu$l of DMEM F/12 medium containing 10% FBS was added to the lower chamber. Then at 24 h, the cells which passed through the membrane were fixed with absolute methanol, stained with 0.5% crystal violet, and quantitated with ImageJ software version 1.48v.

*Western blot analysis*. Cells were lysed with RIPA buffer containing 0.5 M NaF, 0.2 M $NaVO_4$, 1 M Tris-HCl pH 7.5, 0.5 M EDTA, 2.5 M NaCl, 10% (v/v) NP-40, 10% (w/v) SDS, Triton X-100, and protease inhibitor cocktails (Cell Signaling Technology, Inc.). The proteins were quantitated by Bradford kits (Bio-Rad Laboratories Srl.). Sixty micrograms of protein lysates were electrophoresed in 10% SDS-polyacrylamide gel and blotted onto a polyvinylidene fluoride membrane (Bio-Rad Laboratories Srl.). The proteins were blocked in 5% non-fat dried milk diluted in 1X TBS/0.1% Tween-20. Primary antibodies against E-cadherin (1:1,000 dilution, mouse anti-human E-cadherin antibody, 13-1700, Invitrogen; Thermo Fisher Scientific, Inc.), MMP-9 (1:200 dilution, mouse anti-human MMP-9 antibody, 2C3, sc-21733, Santa Cruz Biotechnology, Inc.), MMP-13 (1:100 dilution, rabbit anti-human MMP-13 antibody, H-230, sc-30073, Santa Cruz Biotechnology, Inc.), BAX (mouse anti-human BAX antibody, 1:1,000 dilution, 610983, Becton Dickinson Holdings Pte. Ltd.), BCL-2 (rabbit anti-human BCL-2 antibody, 1:2,000 dilution, ab196495, Abcam) and β-actin (1:10,000 dilution, sc-47778, Santa Cruz Biotechnology, Inc.) were used. The immunoreactive signals were visualized by ECL (Thermo Fisher Scientific, Inc.) under Gel Document Syngene (Syngene). The bands were quantified by ImageJ version 1.48v. β-actin was used as the loading control protein to verify the amount of total loading protein.

*Targeted next-generation sequencing*. The genomic DNA isolation of PC-B-142CA, PC-B-148CA, MDA-MB-231 and MCF-7 was performed using Cobas® DNA sample preparation kit (05985536190, Hoffman-La Roche) according to manufacturer's instructions. The quantity of the extracted DNA samples was determined using the Qubit dsDNA HS Assay Kit (Q32854, Thermo Fisher Scientific, Inc.) and Qubit 2.0 fluorometer (Thermo Fisher Scientific, Inc.). One-hundred nanograms of DNA was used as a template to generate libraries by the GeneRead QIAact AIT DNA UMI Kit (181911, Qiagen) and the GeneRead QIAact BRCA Advanced DNA UMI panel (181925, Qiagen). Sequencing was performed by the GeneReader NGS System (Qiagen). GeneRead UMI Advanced Sequencing Q Kit (185251, Qiagen), GeneRead UMI Advanced Sequencing Q Wash Buffers (185905, Qiagen) were used according to the manufacturer instructions. Single-end sequencing was performed on the GeneReader NGS System (Qiagen). The single-end sequencing was performed. The average read lengths were as follows: MDA-MB-231 [AIT panel: 121.90 base pairs (bps)], MCF-7 (AIT panel: 111.38 bps), PC-B-142CA (AIT panel: 132.57 and BRCA panel:

Table I. Demographic data of the patients and the characteristics of the established cell lines.

| Characteristics | PC-B-142CA | PC-B-148CA |
|---|---|---|
| Patients | | |
| Origin | Breast, metastasis to axilla skin | Breast, right |
| Age (years) | 58 | 50 |
| Sex | Female | Female |
| Tumor size ($cm^3$) | 3.9x3.6x3.0 | 3.5x3.0x3.0 |
| Gross pathology | Angiolymphatic invasion | Angiolymphatic invasion |
| Clinical stage | IV | II |
| ER | Negative | Negative |
| PR | Negative | Negative |
| HER2 | Positive | Negative |
| Ki-67 | Positive | Positive |
| Cell lines | | |
| Growth pattern | Adherent | Adherent |
| Doubling time (h) | 45.0±3.0 | 155.7±5.2 |
| CK | Positive | Positive |
| α-SMA | Negative | Negative |
| FAP | Negative | Negative |
| PD-L1 | Positive | Positive |
| ER | Negative | Negative |
| PR | Negative | Negative |
| HER2 | Positive | Negative |

ER, estrogen receptor; PR, progesterone receptor; HER2, human epidermal growth factor receptor 2; CK, cytokeratin; α-SMA, α-smooth muscle actin; FAP, fibroblast-activation protein; PD-L1, programmed death-ligand 1.

126.73 bps), and PC-B-148CA (AIT panel: 119.04 and BRCA panel: 99.17 bps). Quality control and variant data reviews were performed in Qiagen Clinical Insight Analyze. Qiagen Clinical Insight Interpret software was used for variant interpretation and reporting. The sequences were submitted to GenBank database (https://www.ncbi.nlm.nih.gov/) under the accession number: PRJNA762209 (https://www.ncbi.nlm.nih.gov/sra/PRJNA762209). The BioSample accession numbers were: SAMN21380367, SAMN21380368, SAMN21380369, SAMN21380370, SAMN21380371 and SAMN21380372, respectively.

*Cancer stem cell analysis*. PC-B-142CA and PC-B-148CA cells were harvested and incubated with Allophycocyanin (APC)-labeled anti-CD44 (21270446, ImmunoTools GmbH, Friesoythe Germany, 1:10 dilution) and FITC-labeled anti-CD24 (21270443, ImmunoTools GmbH, 1:10 dilution) antibodies in 1X PBS/2% FBS for 30 min at 4˚C. Mouse IgG1 control FITC-conjugated (21275513, ImmunoTools GmbH) and mouse IgG1 control APC-conjugated (21275516, ImmunoTools GmbH) were used as the isotype controls. The CytoFLEX flow cytometer (Beckman Coulter, Inc.) was used for flow cytometric and data analysis using CytExpert software version 2.1 (Beckman Coulter, Inc.).

*Data collection and statistical analysis*. The values are represented as mean ± standard deviation (SD) from three independent assays. All statistical calculations were performed with the SPSS version 17.0 (SPSS Inc.). The data from two groups were analyzed by paired Student's t-tests and from multiple groups by one-way repeated-measure analysis of variance (ANOVA) followed by Tukey's post-hoc test using GraphPad Prism software version 7.04 (GraphPad Software, Inc.) or SigmaPlot 16.0v (Systat Software, Inc.). $P<0.05$ was considered to indicate a statistically significant difference.

## Results

*Characterizations of PC-B-142CA and PC-B-148CA*. PC-B-142CA cells were isolated from stage IV HER2-positive breast cancer tissues with pathological features of negative ER and PR, positive HER2 (>90%) and Ki-67 (47%). PC-B-148CA was derived from a patient diagnosed with stage II TN breast cancer with negative expression of ER, PR and HER2, but positive Ki-67 (84%) (Table I). Fingerprint results confirmed different origins of these 2 cell lines (Table SI). The PC-B-148CA fingerprint was identical to that of the white blood cells of the patient whose tissue was used to establish PC-B-148CA (data not shown), while that of PC-B-142CA could not be checked due to the unavailability of the sample. The immunocytochemical staining results confirmed PC-B-142CA as a HER2-positive breast cancer cell line, and PC-B-148CA as a TN breast cancer cell line (Table I). PC-B-142CA revealed a great karyotypic heterogeneity with 38 chromosomes with a monosomy X chromosome (Fig. 1A) whereas PC-B-148CA had around 47-58 chromosomes with loss of sex chromosomes

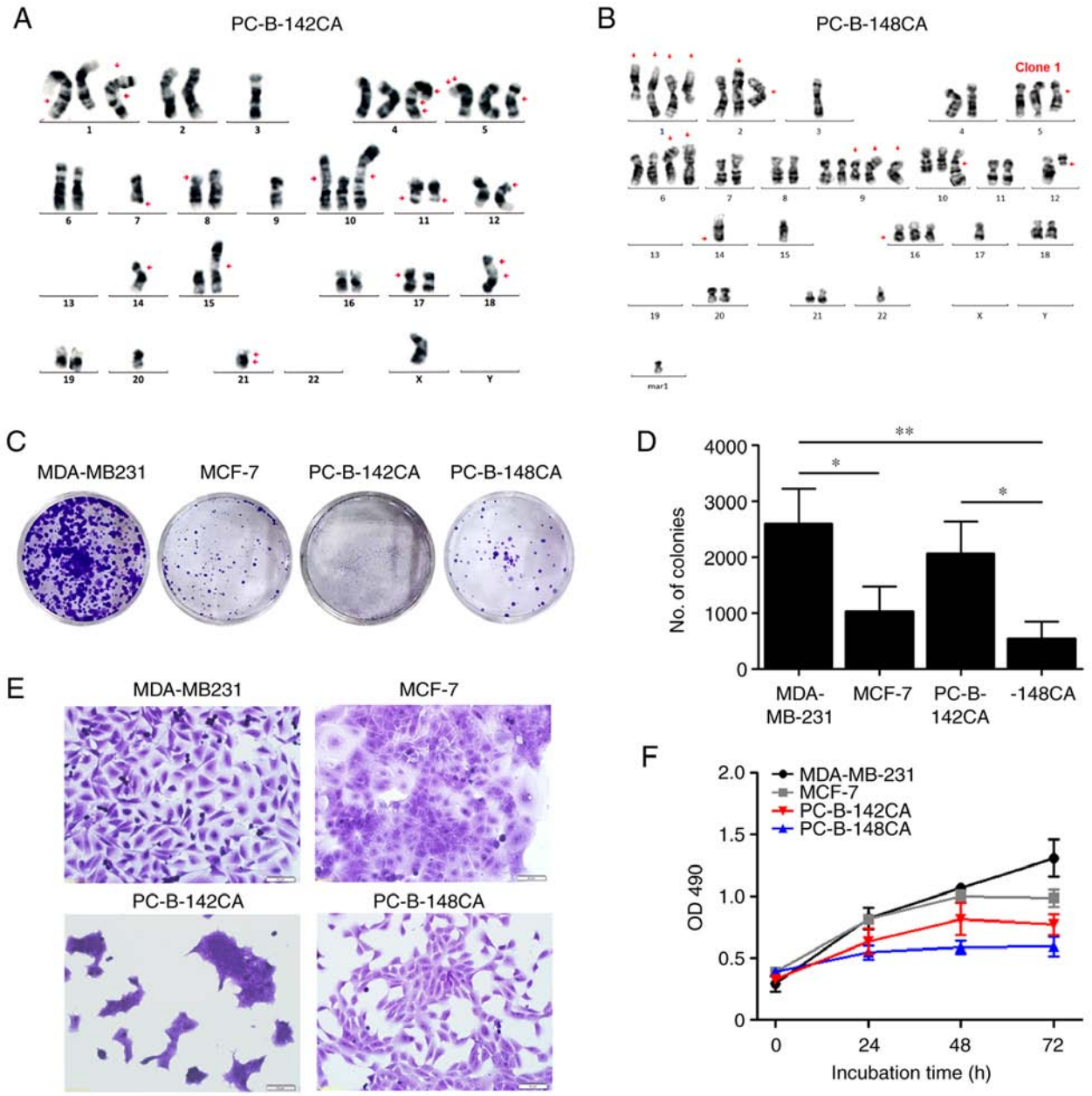


Figure 1. Characterization of PC-B-142CA and PC-B-148CA cell lines. (A) Chromosomal pattern and growth properties of the two in-house established breast cancer cell lines. The karyotype of PC-B-142CA (A) and PC-B-148CA (B) cells. (C) Proliferation properties of breast cancer cells by clonogenic assay staining with 0.5% crystal violet was performed at day 10 after seeding. (D) The colony numbers were counted by photometric measurements using the CellCounter software version 0.2.1. Three independent experiments were performed. (E) The morphology of cells under a phase contrast light microscopy with 0.5% crystal violet staining; scale bars, 20 $\mu$m. (F) Growth curve analysis by counting viable cell numbers using the MTS assay at 0, 24, 48 and 72 h. $^{*}$P<0.05; $^{**}$P<0.01.

and several numerical and structural rearrangements and unidentifiable aberrations (Figs. 1B and S1).

The colony formation assay exhibited that TN PC-B-148CA had a significantly slower growth rate than the commercial TN MDA-MB-231 (Fig. 1C and D). PC-B-142CA formed a colony faster than PC-B-148CA, but slower that MDA-MB-231. PC-B-142CA had a very small size and grew in cluster of cells, whereas PC-B-148CA showed a polygonal shape (Fig. 1E). The growth rates of PC-B-142CA and PC-B-148CA were lower than those of MDA-MB-231 and MCF-7 (Fig. 1F). PC-B-148CA had the slowest growth rate among these four cells with a doubling time of 155.7±5.2 h, while that of PC-B-142CA was 45.0±3.0 h (Table I).

*Morphology and cellular markers of PC-B-142CA and PC-B-148CA*. PC-B-142CA cells adhered to form a big tight colony with blurred cell borders (Fig. 2A, bright field), while PC-B-148CA exhibited characteristic of spindle shape with multiple processes and seldom multinucleated cells (Fig. 2C, bright field). PC-B-148CA had a bigger cell size than PC-B-142CA. Both cells were positive for all CKs but no α-SMA and FAP fibroblast markers were detected (Fig. 2A and C). PD-L1 was found in both PC-B-142CA and PC-B-148CA. The immunocytochemistry staining confirmed positive expression of HER2 in PC-B-142CA, whereas negative ER, PR and HER2 were detected in PC-B-148CA (Fig. 2A and C). The 3-D spheroid of PC-B-142CA was larger

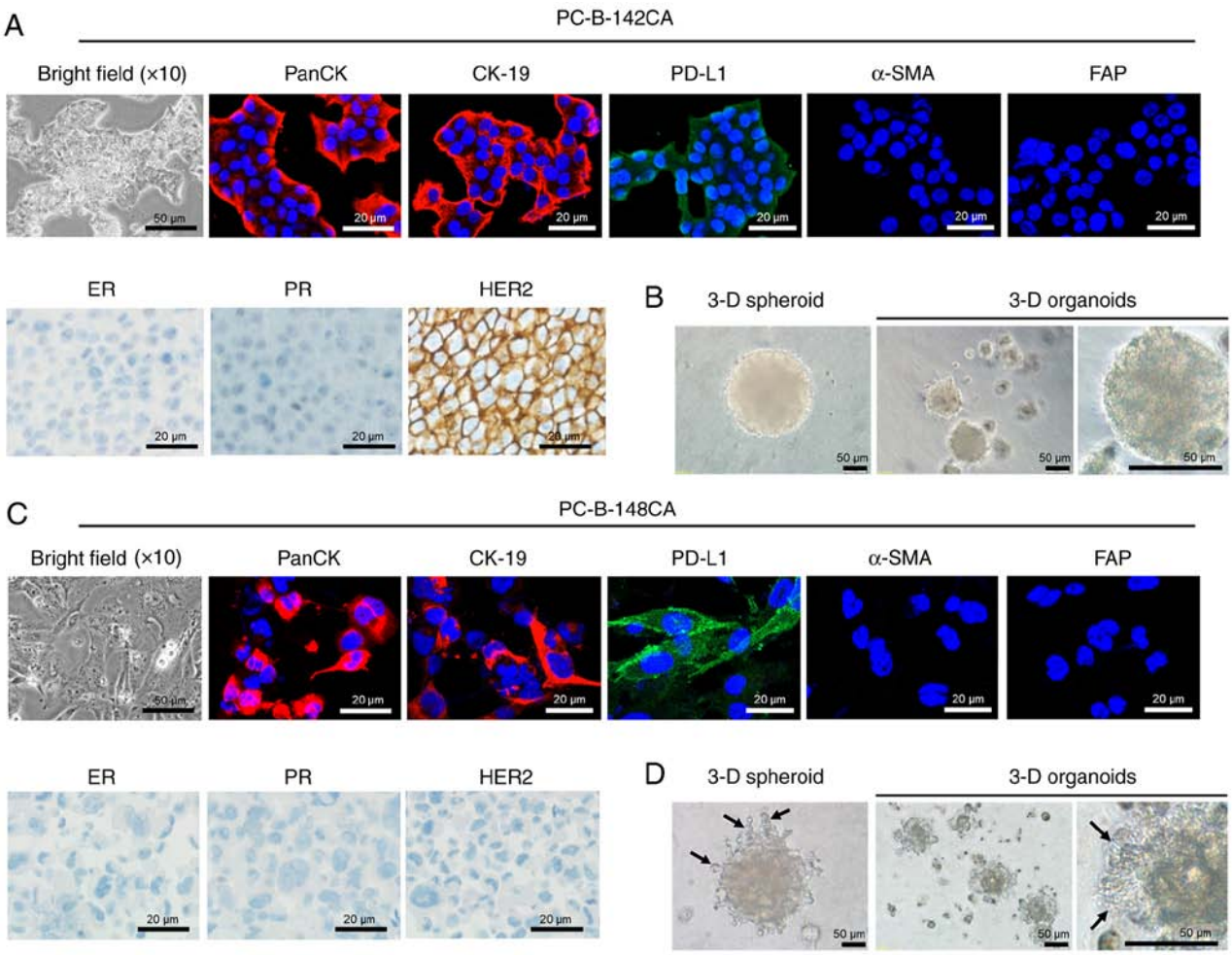


Figure 2. Morphology of the in-house breast cancer cells. (A) PC-B-142CA and (C) PC-B-148CA cell lines. Typical morphology of stable culture cells under a phase contrast light microscopy (x200 magnification; scale bars, 50 $\mu$m). (Top panels) Expression of biological markers of epithelial cells by immunofluorescence staining of PanCK (red fluorescence), CK-19 (red fluorescence), PD-L1 (green fluorescence), α-SMA (red fluorescence) and FAP (green fluorescence); images captured at x400 magnification; scale bars, 20 $\mu$m. Staining with Hoechst33342 (blue fluorescence) was conducted to visualize chromatin. (Lower left panels) Phase-contrast micrographs showing the immunohistochemistry staining of ER, PR and HER2; scale bars, 20 $\mu$m. (B and D) The 3-D formation ability is shown by 3-D spheroids at day 5 and 3-D organoids at day 14. Invadopodia were observed in only 3-D PC-B-148CA cells (black arrow). CK, cytokeratin; PD-L1, programmed death-ligand 1; α-SMA, α-smooth muscle actin; FAP, fibroblast-activation protein; ER, estrogen receptor; PR, progesterone receptor; HER2, human epidermal growth factor receptor 2.

than that of PC-B-148CA (Fig. 2B and D). The 3-D mean diameter continuously increased with time from 0.048±0.04 $\mu m^3$ at day 0 to 0.118±0.21 $\mu m^3$ at day 5 for PC-B-142CA and from 0.021±0.04 $\mu m^3$ at day 0 to 0.095±0.058 $\mu m^3$ at day 5 for PC-B-148CA. The aggregation and compaction of 3-D organotypic modeling was observed at day 14 of culture. The 3-D organoids of PC-B-142CA exhibited a round shape with smooth surface, whereas those of PC-B-148CA had invadopodia representing the specialized adhesive structures capable to invade surrounding tumor microenvironment. This similar feature was also observed in the PC-B-148CA spheroid.

*Migration and cancer stem cell properties of PC-B-142CA and PC-B-148CA*. MBA-MB-231 TN breast cancer cells confirmed their most rapid migration by wound healing and Transwell migration assays in 10% FBS media (Fig. 3A and D). The results showed that PC-B-148CA closed a 70% wound gap at 24 h (Fig. 3A and C), while at this time point, PC-B-142CA had only 30% wound closure and needed more than 96 h to completely heal the wound gap (data not shown). We tried to culture it in serum free, unluckily, the cells did not grow confluently and we could not do wound scratching. The primary cells did not tolerate serum starving as well as the established cell lines, hence wound healing assay in our experiment was performed in the presence of serum. The doubling times of PC-B-142CA and PC-B-148CA were approximately 45±3.0 and 155.7±5.2 h, respectively, implying that within 24 h of this assay, cells did not proliferate. The Transwell migration assay essentially confirmed the migration capability observations from high to low as: MBD-MB-231>PC-B-148CA>MCF-7>PC-B-142CA (Fig. 3D). The western blot analysis of the proteins involved in cancer cell migration exhibited that E-cadherin was basally expressed in all 4 cell lines in this study and showed the highest level in MCF-7, especially, the 120-kDa mature isoform whereas MMP-9 and MMP-13 were markedly higher in MDA-MD-231 and PC-B-148CA cells (Fig. 3E-H).

$CD24^-/CD44^+$ representing cancer stem cells (CSCs) of breast cancer, were detected in PC-B-142CA and PC-B-148CA as 8.75 and 96.9% (Fig. 3I and J). MDA-MB-231 had around 98.1% CSCs, while that of MCF-7 was 65.0%.

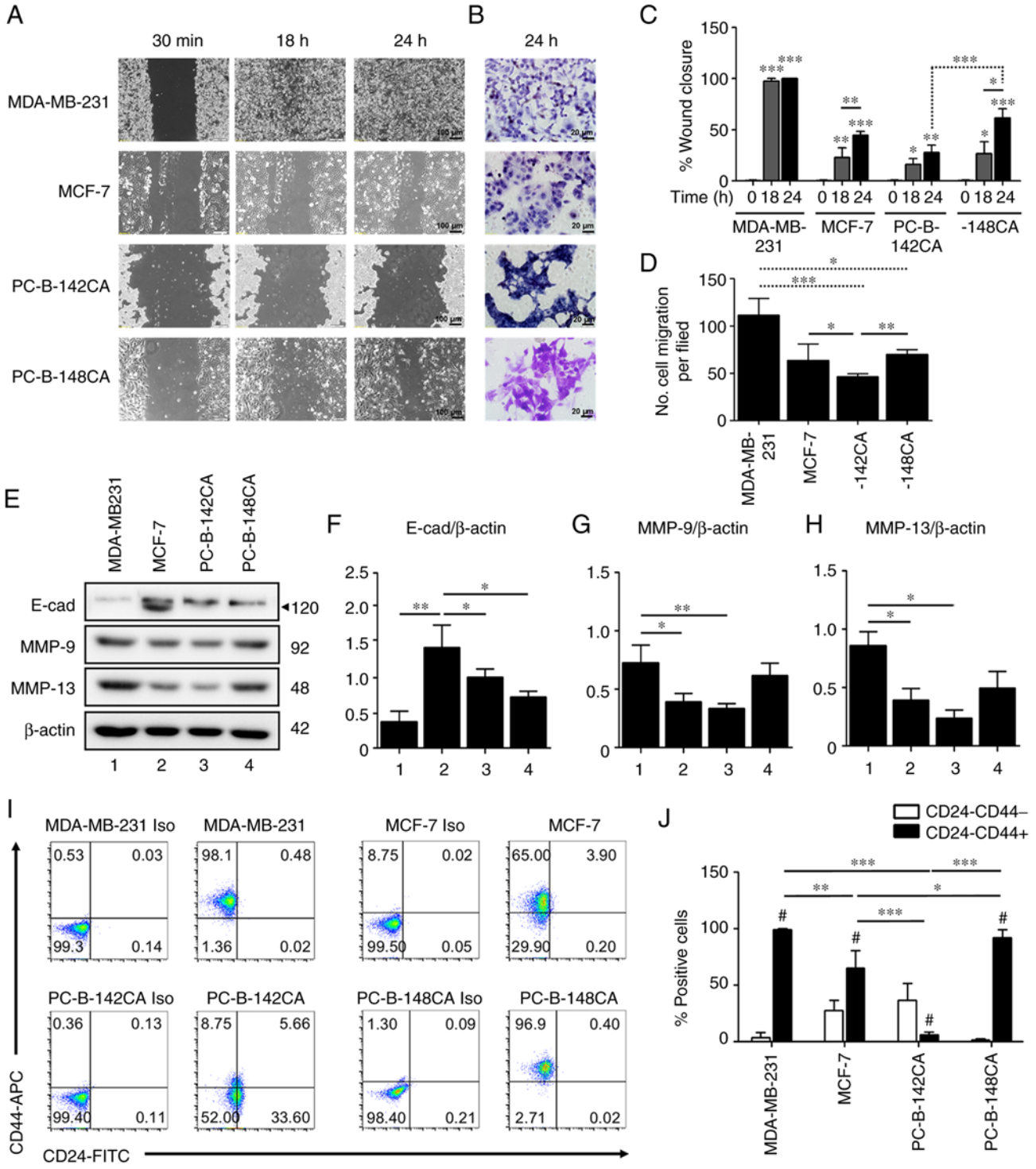


Figure 3. Migration ability of PC-B-142CA and PC-B-148CA cells compared to commercial MDA-MB-231 and MCF-7 cell lines. (A) The migration assay was performed by scratch wound assay at 30 min, 18 h and 24 h after incubation, and (B) Transwell migration assay at 24 h. Representative images captured at x400 magnification; scale bar, 20 $\mu$m, are shown. (A and C) Photographs of scratch wound were taken and the width of the wound area was measured at the indicated times. The graphs report the rate of wound healing (%) for each time point estimated using ImageJ software. Data represent the average ± SD wound calculated for three different fields per each condition in three independent experiments. (D) Quantitation of the migratory cells in 5 fields randomly chosen was performed with ImageJ. Data represent the number of migrated cells in triplicate. (E) Western blot analysis of E-cadherin, MMP-9 and MMP-13 proteins in different breast cancer cells. β-actin was used as a loading control. (F-H) Densitometry data from three separate experiments, expressed as mean ± standard deviation (SD) are shown in the histograms. (I and J) Flow cytometry analysis of PC-B-142CA and PC-B-148CA cells using CD44 and CD24 markers. MDA-MB-231 and MCF-7 were used as control. An isotype (Iso) was used as a control to each cell line. #Compared to the CD24-CD44- population. *P<0.05, **P<0.01, ***P<0.001. MMP, matrix metalloproteinase.

*DOX and PTX resistance of PC-B-142CA and PC-B-148CA.* To determine the relevant toxic concentration of DOX and PTX, the breast cancer cells were exposed to the increasing concentrations of DOX and PTX (0.01, 0.1, 1 and 10 $\mu$M) and cell viability was assayed at 24, 48, 72 and 96 h. In 2-D culture, 0.01 $\mu$M of DOX (Fig. 4C) or 1 $\mu$M of PTX (Fig. 4D)

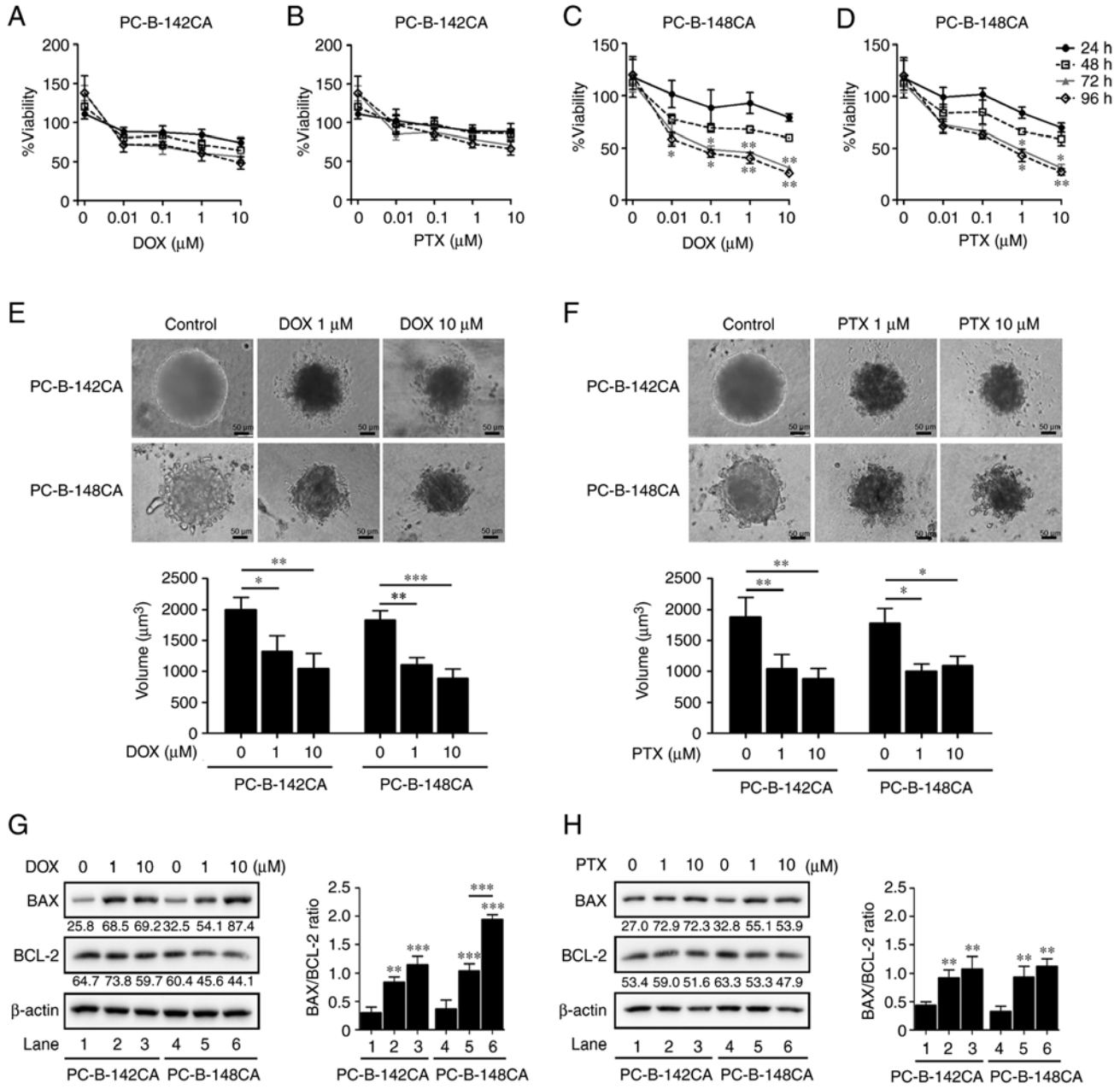


Figure 4. DOX and PTX induce cell death in PC-B-142CA and PC-B-148CA cells. (A) PC-B-142CA and (C) PC-B-148CA cells were plated and exposed to 0, 0.01, 0.1, 1 and 10 $\mu$M of DOX and (B) PC-B-142CA and (D) PC-B-148CA cells were treated with 0, 0.01, 0.1, 1 and 10 $\mu$M of PTX for 24, 48, 72 and 96 h (0 h was used as the normalization). Quantitative results of MTS staining were performed in triplicate. (E and F) Phase-contrast micrographs showing the morphology of 3-D sphere-formation of two breast cancer cell lines tested with 0, 1 and 10 $\mu$M of DOX (E) and of PTX (F) were tested for 72 h (day 7 of culture). Images were captured at x200 magnification; scale bar, 50 $\mu$m. (G and H) Expression of BAX and BCL-2 in PC-B-142CA and PC-B-148CA treated or not with 0, 1 and 10 $\mu$M of DOX (G) and of PTX (H) for 72 h. β-actin was used as protein loading control. Densitometry analysis of the relative band intensity of the western blotting. $^{*}$P<0.05; $^{**}$P<0.01 and $^{***}$P<0.001 compared with the untreated control. DOX, doxorubicin; PTX, paclitaxel.

was the minimum concentration which elicited the highest toxic effect in PC-B-148CA cells, whereas no cytotoxic effect was found in the PC-B-142CA cell line (Fig. 4A and B). Interestingly, 3-D spheroid formation showed that after exposure to 1 $\mu$M DOX and 10 $\mu$M PTX, the size of tumor spheroids was significantly reduced from the control without drug treatment in PC-B-142CA and PC-B-148CA cells at 72 h (Fig. 4E and F). Moreover, DOX and PTX-treated PC-B-142CA and PC-B-148CA increased the pro-apoptotic BAX protein, while decreased the expression of the anti-apoptotic BCL-2 protein (Fig. 4G and H).

*Mutation of the drug-targeted genes*. Drug-targeted gene mutations were checked in the PC-B-142CA and PC-B-148CA cells in comparison to those in the MDA-MB-231 and MCF-7 cells (Table II). The pathogenic mutations represented the variants well established as disease causing including *KIT* (E839K, 50.0%), *PIK3CA* (C420R, 68.0%), *SMAD4* (Q224*, 100.0%, * represented stop codon), and *TP53* loss-of-function (I202T, 98.0%) were detected in PC-B-142CA, whereas *BRCA2* (T3033fs*11, 16.0%) and *TP53* (R196*, 100%) loss-of-function, and *NRAS* gain-of-function (G12C, 35.0%) were found in PC-B-148CA. *ERBB2* amplification and

Table II. The drug-targeted gene alterations in the breast cancer cell lines.

| Gene | Exon | Nucleotide alteration | Amino acid variant | % Mutation (Pathogenic[a]) | | | |
|---|---|---|---|---|---|---|---|
| | | | | MCF-7 | MDA-MB-231 | PC-B-142CA | PC-B-148CA |
| ALK | 29 | c.4587C>G | p.D1529E | WT | 62.49% | 33% | 31% |
| ALK | 29 | c.4472A>G | p.K1491R | WT | 64.03% | 33% | 32% |
| ALK | 29 | c.4381A>G | p.I1461V | 99% | 99.03% | 99% | 99% |
| ALK | 23 | c.3600G>C | p.A1200A | WT | WT | WT | 34% |
| ALK | 18 | c.3036G>A | p.T1012T | WT | WT | 65% | WT |
| ALK | 15 | c.2535T>C | p.G845G | 100% | WT | 65% | WT |
| ALK | 2 | c.702T>A | p.P234P | 100% | 66.88% | 68% | 100% |
| ALK | 1 | c.27C>G | p.L9L | 100% | 100% | 100% | 100% |
| PIK3CA | 1 | c.-77+8483C>T | - | WT | 28.28% | WT | WT |
| PIK3CA | 1 | c.-76-23509A>G | - | WT | 30.66% | WT | WT |
| PIK3CA | 10 | c.1633G>A | p.E545K | 58%[a] | WT | WT | WT |
| PIK3CA | 8 | c.1258T>C | p.C420R | WT | WT | 68%[a] | WT |
| FGFR3 | 14 | c.1953G>A | p.T651T | 100% | 99.15% | 99% | 100% |
| PDGFRA | 7 | c.939T>G | p.G313G | WT | 35.17% | 48% | WT |
| PDGFRA | 10 | c.1432T>C | p.S478P | WT | 30.59% | WT | WT |
| PDGFRA | 12 | c.1701A>G | p.P567P | 99% | 99.44% | 100% | 100% |
| PDGFRA | 13 | c.1809G>A | p.A603A | WT | 35.37% | WT | WT |
| PDGFRA | 18 | c.2472C>T | p.V824V | WT | 34.80% | WT | WT |
| KIT | 16 | c.2362-77G>A | - | WT | 36.76% | WT | WT |
| KIT | 18 | c.2586G>C | p.L862L | WT | 34.51% | WT | WT |
| KIT | 18 | c.2515G>A | p.E839K | WT | WT | 50%[a] | WT |
| EGFR | 4 | c.474C>T | p.N158N | 100% | 25% | WT | 100% |
| EGFR | 13 | c.1562G>A | p.R521K | WT | WT | 100% | WT |
| EGFR | 16 | c.1968C>T | p.H656H | 83% | WT | WT | 49% |
| EGFR | 18 | c.2184+19G>A | - | 78% | WT | WT | 48% |
| EGFR | 20 | c.2361G>A | p.Q787Q | 99% | 98.77% | WT | 48% |
| EGFR | 25 | c.2982C>T | p.D994D | 83% | WT | 34% | 100% |
| BRAF | 15 | c.1805C>G | p.S602C | WT | WT | 45.00% | WT |
| BRAF | 16 | c.1929A>G | p.G643G | WT | 99.36% | 100% | WT |
| BRAF | 11 | c.1391G>T | p.G464V | WT | 96.08%[a] | WT | WT |
| KRAS | 5 | c.*2505T>G | - | 31% | WT | WT | WT |
| KRAS | 2 | c.38G>A | p.G13D | WT | 98.83%[a] | WT | WT |
| ERBB2 | - | - | - | WT | WT | Amplificationa | WT |
| ERBB2 | 27 | c.3508C>G | p.P1170A | 99% | 98.51% | 3.77% | WT |
| ERBB2 | 17 | c.1960A>G | p.I654V | 100% | WT | WT | WT |
| ERBB2 | 17 | c.1963A>G | p.I655V | 100% | WT | WT | WT |
| ERBB2 | 27 | c.3631C>G | p.P1211A | WT | WT | 3.67% | WT |
| ERBB2 | 27 | c.3651C>T | p.F1217F | WT | WT | 4.21% | WT |
| ERBB3 | 27 | c.3355A>T | p.S1119C | WT | WT | WT | 99% |
| ESR1 | 10 | c.1782G>A | p.T594T | 65% | WT | WT | 56% |
| ESR1 | 3 | c.30T>C | p.S10S | 23% | WT | 100% | WT |
| MAP2K2 | 2 | c.192C>T | p.V64V | WT | 53.04% | WT | WT |
| MET | 20 | c.3912C>T | p.D1304D | 49% | WT | 99% | 67% |
| NOTCH1 | 27 | c.5094C>T | p.D1698D | 43% | WT | 99% | 99% |
| SMAD4 | 6 | c.670C>T | p.Q224* | WT | WT | 100%[a] | WT |
| BRCA1 | 10 | c.2612C>T | p.P871L | ND | ND | 93% | WT |
| BRCA2 | 10 | c.1274C>G | p.S425C | ND | ND | 99% | WT |
| BRCA2 | 10 | c.1114A>C | p.N372H | ND | ND | WT | 99% |

Table II. Continued.

| | | | | | | | |
|---|---|---|---|---|---|---|---|
| BRCA2 | 11 | c.4563A>G | p.L1521L | ND | ND | WT | 100% |
| BRCA2 | 11 | c.6513G>C | p.V2171V | ND | ND | WT | 99% |
| BRCA2 | 14 | c.7397T>C | p.V2466A | ND | ND | WT | 100% |
| BRCA2 | 17 | c.7806-14T>C | - | ND | ND | 100% | WT |
| BRCA2 | 23 | c.9097dupA | p.T3033fs*11 | ND | ND | WT | 16%[a] |
| TP53 | 6 | c.586C>T | p.R196* | ND | ND | WT | 100%[a] |
| TP53 | 8 | c.839G>A | p.R280K | ND | ND | WT | WT |
| TP53 | 4 | c.215C>G | p.P72R | ND | ND | WT | WT |
| TP53 | 7 | c.695T>C | p.1232T | ND | ND | 98%[a] | WT |

*, stop codon; -, not found; WT, wild-type; ND, not done. [a]Pathogenic mutation: the variant which is considered and well established as disease causing. *ALK*, anaplastic lymphoma kinase; *PIK3CA*, phosphatidylinositol 3-kinase, catalytic subunit α; *FGFR3*, fibroblast growth factor receptor 3; *PDGFRA*, platelet derived growth factor receptor α; *KIT*, proto-oncogene, also known asc-Kit; *EGFR*, epidermal growth factor receptor; *ERBB2*, Erb-B2 receptor tyrosine kinase 2, also known as HER2/neu; *ERBB3*, Erb-B2 receptor tyrosine kinase 3; *ESR1*, estrogen receptor 1; *MAP2K2*, mitogen-activated protein kinase kinase 2; *MET*, MET proto-oncogene; receptor tyrosine kinase; *NOTCH1*, Notch receptor 1; *SMAD4*, SMAD family member 4; BRCA1/2, breast cancer 1/2.

*PIK3CA* mutation at exon 8 (c.1258T>C, 68%) were found in PC-B-142CA.

## Discussion

The incidence of breast cancer in females is increasing worldwide (3). Luminal breast cancer is the most common subtype whereas HER2-positive is the second most common (6). High local recurrence and bone metastasis in patients with luminal breast cancer is commonly detected during a 2- to 5-year period (15). The median overall survival for metastatic TN breast cancer is approximately 1 year compared to approximately 5 years for the other 2 subtypes (6). Moreover, drug resistance is common in all breast cancer types despite the different treatment modalities applied (16). Several breast cancer cell lines are existing and widely used in research fields. In the present work, two novel cell lines from tumor tissues of two breast cancer patients diagnosed with HER2-positive and triple-negative (TN) breast cancer were established and designated as PC-B-142CA and PC-B-148CA. The characterization for their biological, molecular, and genetic properties confirmed that PC-B-148CA had high aggressive properties including migration, doxorubicin (DOX)/paclitaxel (PTX) resistance and stemness properties, whereas HER2-positive PC-B-142CA had pathogenic gene mutations related to the resistance to several chemotherapeutic drugs.

Both PC-B-142CA and PC-B-148CA cell lines grew as adherent monolayer cells with morphology of epithelial cells. The PC-B-142CA proliferation rate doubling time compared to PC-B-148CA was around 45 vs. 155 h. The presence of fibroblast-activation protein (FAP) and α-smooth muscle actin (α-SMA) confirmed the characteristic of cancer-associated fibroblasts (17), whereas the presence of cytokeratin (CK) represented cancer cells (18). Thus, having negative α-SMA and FAP, with positive CK ensures the purity of PC-B-142CA and PC-B-148CA without fibroblast contamination. The expression of programmed death-ligand 1 (PD-L1) in both PC-B-142CA and PC-B-148CA cell lines implies the ability of these cells to resist T cell killing as PD-L1 is a checkpoint molecule acting as a break to inhibit T cell function (19,20). Atezolizumab, an anti-PD-L1 antibody, has just been approved by the US Food and Drug Administration (US FDA) for use in combination with chemotherapy for the treatment of patients with PD-L1-positive, non-operable, locally advanced/metastatic TN breast cancer (21). Hence, PD-L1-expressing PC-B-142CA and PC-B-148CA cells may be a valuable aid in the search to overcome immune checkpoint-mediated T cell dysfunction in breast cancer.

It is widely acknowledged that cancer stem cells (CSCs) serve as an important part in the occurrence and development of tumors on account of their ability for self-renewal, differentiation, proliferation and induction of tumor growth (22,23). Surface CD44, overexpressed in several types of cells, is a cell-surface glycoprotein involved in tumorigenesis, metastasis and recurrence (24,25). PC-B-148CA showed the highest stemness property. TN breast cancer cell lines including MDA-MB-231, MDA-MB-436, Hs578T, SUM1315 and HBL-100 with a higher percentage of $CD44^+/CD24^-$ cells (>30%) express higher levels of pro-invasive genes and are highly invasive (26). PC-B-148CA cells showed marked migration activity when compared to the PC-B-142CA cells. This property was found to be correlated with the histological data of the tissue of origin of PC-B-148CA cells including invasive lobular carcinoma and angiolymphatic invasion. Serum starving is the most common non-pharmaceutical method for minimizing proliferation in wound healing assays, but the degree of serum starving has to be calculated for each cell type under investigation (27). Please note that primary cells do not tolerate serum starving as well as established cell lines. PC-B-142CA and PC-B-148CA cells were tested for their migration capability in the presence of serum. Hence, the proliferation parameter cannot be ruled out from this assay results.

Metastatic cancer cells invade surrounding tissues and blood vessels by forming F-actin-rich protrusions known as invadopodia, which degrade the extracellular matrix and enable invasion of tumor cells (28). The proportion of $CD44^+/CD24^-$ in breast cancer cell populations has been reported to enrich

mammosphere formation (29) and tumorigenesis in mice (30) and have been well studied (31). Invadopodia were observed in PC-B-148CA cells forming as 3-D structures, both spheroid and organoid. A key step in tumor progression is the transition of stationary epithelial cells to become motile by the loss of cell-cell adhesion and matrix degradation. The process of epithelial-mesenchymal transition (EMT) exhibits molecular hallmark by downregulation of E-cadherin (26,32). The phenotype of cell migration was consistent with the western blot analysis which revealed low expression of E-cadherin in the PC-B-148CA cells. All of these characteristics support the high invasive property of PC-B-148CA cells. However, MCF-7 cells have a high E-cadherin, yet a high migration rate was detected. This may be explained by the fact that not only the E-cadherin level reflects the migration ability, but also other proteins such as matrix metalloproteinases (MMPs) and N-cadherin were previously found with high levels in MCF-7 cells (33,34). In breast cancer, overexpression of several MMPs has been reported which is generally associated with breast tumor progression. MMP-9 is a potential biomarker which is widely found to play a role in tumor invasion, metastasis and angiogenesis and to mediate tumor microenvironment (35). MMP-9 protein expression in MDA-MB-231 and MCF-7 cells was found to be significantly higher than in normal breast cells (36). Since MMP-13 is expressed in a broad range of breast cancer cells, it has emerged as a novel metastatic biomarker. MDA-MB-231 breast cancer cells that secrete higher levels of MMP-13 are less aggressive than MCF7 cells (37). Consistent with our results, MMP-9 and MMP-13 were highly expressed in MDA-MB-231, MCF-7 and PC-B-148CA cells when compared with these levels in PC-B-142CA cells. The lack of N-cadherin expression assessment is a limitation of this study.

The 3-D spheroid and 3-D organoid models enable mimicking of the *in vivo* tumor condition in patients (38). Both PC-B-142CA and PC-B-148CA cell lines showed the capability of producing 3-D multicellular tumor spheroids and 3-D tumor organoids. Additionally, cells within tumor spheroids may have activities similar as that in a patient's body, promotion of migration and invasion; such features are absent in 2D culture. The different sensitivity to DOX or PTX was detected in these two cell lines. DOX and PTX had a strong impact on the spheroid size of both PC-B-142CA and PC-B-148CA cell lines, with small size and outer loose layer of sphere cells in a dose-dependent manner.

In the mutation analysis, *ERBB2* (a gene encoding the HER2 protein) amplification found in PC-B-142CA cells was consistent with the presence of HER2 by an immunocytochemistry result and confirmed that it had originated from HER2-positive breast cancer tissue. Five mutations of drug-targeted genes including *KIT*, *PIK3CA*, *SMAD4* and *TP53* found in PC-B-142CA together with the *ERBB2* amplification are related to the resistance of several targeted drugs. Amplification of *HER2* together with *PIK3CA* may aggravate the resistance to HER2-targeted drugs and suggest the combination of treatment with PI3K inhibitors (16). Multiple advances in the treatment of HER2-positive breast cancer due to multiple mutated genes were found leading to the benefit of the combination of HER2 and targeted inhibitors. *PI3KCA* mutant HER2-positive bearing mice demonstrated tumor regression after combined lapatinib and trastuzumab treatment (39). Further studies using PC-B-142CA as a model of drug resistance may be valuable for identification of better targeted molecules in HER2-positive breast cancer.

As to the review of literature, the well-known HER2-positive breast cancer cell lines are the cells with *HER2* gene overexpression and more aggressive phenotypes. In comparison to these existing cell lines, the newly established PC-B-142CA cell line exhibited *BRCA1* and *BRCA2* mutations. *BRCA1* mutation at exon 10 (c.2612C>T) was found in PC-B-142CA (93%) cells and the *BRCA2* mutation showed in exon 10 (c.12740C>G, 99%) and exon 17 (c.7806-14T>C, 100%). Commercial HER2-positive cell lines including AU565, HCC1569, HCC1954, HCC202, KPL-4, OCUB-F, SKBR3, SKBR5, SUM190PT, SUM225CWN and UACC893 cells have wild-type *BRCA1* (12,40,41). The breast cancer susceptibility genes, BRCA1 and BRCA2, are critically involved in the repair of DNA double-strand breaks (42) and drug resistance in cancer treatment (43). The *BRCA1* and *BRCA2* mutations showed an association with the development of breast cancer (44), ovarian cancer (45), prostate cancer (46) and pancreatic cancer (47). The BRCA1/2-mutated PC-B-142CA cells can be used in the area of breast cancer research for insight into the effect of BRCA aberration in breast cancer progression.

Moreover, *ERBB2* amplification was found in HER2-positive PC-B-142CA cells which may be related to drug resistance of anastrozole, anthracycline, capecitabine, docetaxel/trastuzumab, exemestane, fulvestrant, lapatinib, lapatinib/letrozole, lapatinib/trastuzumab, letrozole, neratinib, pertuzumab, pertuzumab/trastuzumab, tamoxifen and trastuzumab/emtansine; whereas *PIK3CA* mutation at exon 8 (c.1258T>C) is a pathogenic mutation correlated with alpelisib and combined alpelisib/fulvestrant resistance.

In the PC-B-148CA cell line, the gain-of-function mutation of NRAS (G12C) leads to NRAS activation involving the RAS/RAF/MARK/PI3K pathway resulting in drug resistance (48). In addition, the loss-of-function mutations of *BRCA2* (16%) and *TP53* (100%) were found in PC-B-148CA cells, which is common in tumorigenesis (49,50). Loss of TP53 is common in advanced cancers; *TP53* exon 6 single nucleotide variant mutant displays a relationship in promoting cancer cell proliferation, survival and EMT features (51,52). In comparison to *TP53* mutations in MDA-MB-231 cells, over 90% of the mutations in *TP53* in MDA-MB-231 were found at exons 8 (codon 280: Arg>Lys (R280K) (53), that indicates the impact of mutant TP53 upon the tumorigenic properties of MDA-MB-231 cell by loss of cytoplasmic pro-apoptotic activity (54). There are no mutations of *TP53* in MCF-7 cells (53,55).

In conclusion, this study established two breast cancer cell lines from HER2-positive and TN breast cancer cell lines and characterized their tumorigenic phenotypes including cell growth, migration and DOX/PTX responses and targeted drug-related gene aberrations. PC-B-142CA cells can serve as a novel HER2-positive cell line for drug resistance and unravelling the effect of BRCA aberration in breast cancer progression, while PC-B-148CA is a novel TN cell line suitable for invasive and stemness-related properties. Further *in vivo* study on these two breast cancer cells, such as tumor biology, cellular and molecular carcinogenesis and drug response, are needed. Importantly, these novel breast cancer cell lines represent valuable tools in breast cancer research.

**Acknowledgements**

The authors would like to thank Professor James A. Will, University of Wisconsin-Madison, USA for the English edition.

**Funding**

This study was funded by the National Research Council of Thailand (NRCT), Ministry of Higher Education, Science, Research and Innovation (grant no. RSA6280091) Thailand and Research Grant, Faculty of Medicine Siriraj Hospital, Mahidol University (R016033015) to CT.

**Availability of data and materials**

All data generated or analyzed during this study are included in this published article. Other related data can be available upon request to the authors.

**Authors' contributions**

ST, PT, PTY, NP and CT designed the experiments; ST performed the main research work. PJ, JP and NS prepared the samples for the experiments. MW, DSN and POC acquired the patient breast cancer tissues and analyzed the results. ST analyzed and interpreted all the data, prepared figures/tables and wrote the manuscript, and finally submitted the manuscript. CT performed the research grant application, wrote and improved the scientific quality of the manuscript, and finally submitted the manuscript. All authors read and approved the manuscript and agreed to be accountable for all aspects of the research in ensuring that the accuracy or integrity of any part of the work.

**Ethics approval and consent to participate**

All experimental procedures performed in the present study were approved by Siriraj Institutional Review Board (COA no. Si 329/2017) and written informed consent was provided by the subjects. All patients recruited in this study were accepted for information of the study by written informed consent.

**Patient consent for publication**

Not applicable.

**Competing interests**

The authors declare that they have no competing interests.

**References**

1. Ghoncheh M, Pournamdar Z and Salehiniya H: Incidence and mortality and epidemiology of breast cancer in the world. Asian Pac J Cancer Prev 17: 43-46, 2016.
2. Torre LA, Bray F, Siegel RL, Ferlay J, Lortet-Tieulent J and Jemal A: Global cancer statistics, 2012. CA Cancer J Clin 65: 87-108, 2015.
3. Siegel RL, Miller KD and Jemal A: Cancer statistics, 2019. CA Cancer J Clin 69: 7-34, 2019.
4. Alanazi IO and Khan Z: Understanding EGFR signaling in breast cancer and breast cancer stem cells: Overexpression and therapeutic implications. Asian Pac J Cancer Prev 17: 445-453, 2016.
5. Tang Y, Wang Y, Kiani MF and Wang B: Classification, treatment strategy, and associated drug resistance in breast cancer. Clin Breast Cancer 16: 335-343, 2016.
6. Waks AG and Winer EP: Breast cancer treatment: A review. JAMA 321: 288-300, 2019.
7. Elstrodt F, Hollestelle A, Nagel JH, Gorin M, Wasielewski M, van den Ouweland A, Merajver SD, Ethier SP and Schutte M: BRCA1 mutation analysis of 41 human breast cancer cell lines reveals three new deleterious mutants. Cancer Res 66: 41-45, 2006.
8. Neve RM, Chin K, Fridlyand J, Yeh J, Baehner FL, Fevr T, Clark L, Bayani N, Coppe JP, Tong F, *et al*: A collection of breast cancer cell lines for the study of functionally distinct cancer subtypes. Cancer Cell 10: 515-527, 2006.
9. Sharieh EA, Awidi AS, Ahram M and Zihlif MA: Alteration of gene expression in MDA-MB-453 breast cancer cell line in response to continuous exposure to Trastuzumab. Gene 575: 415-420, 2016.
10. Hámori L, Kudlik G, Szebényi K, Kucsma N, Szeder B, Póti Á, Uher F, Várady G, Szüts D, Tóvári J, *et al*: Establishment and characterization of a brca1$^{-/-}$, p53$^{-/-}$ mouse mammary tumor cell line. Int J Mol Sci 21: 1185, 2020.
11. Han Y, Nakayama J, Hayashi Y, Jeong S, Futakuchi M, Ito E, Watanabe S and Semba K: Establishment and characterization of highly osteolytic luminal breast cancer cell lines by intracaudal arterial injection. Genes Cells 25: 111-123, 2020.
12. Dai X, Cheng H, Bai Z and Li J: Breast cancer cell line classification and its relevance with breast tumor subtyping. J Cancer 8: 3131-3141, 2017.
13. Goldhirsch A, Winer EP, Coates AS, Gelber RD, Piccart-Gebhart M, Thürlimann B and Senn HJ; Panel members: Personalizing the treatment of women with early breast cancer: Highlights of the St Gallen international expert consensus on the primary therapy of early breast cancer 2013. Ann Oncol 24: 2206-2223, 2013.
14. Prat A, Cheang MC, Martín M, Parker JS, Carrasco E, Caballero R, Tyldesley S, Gelmon K, Bernard PS, Nielsen TO and Perou CM: Prognostic significance of progesterone receptor-positive tumor cells within immunohistochemically defined luminal A breast cancer. J Clin Oncol 31: 203-209, 2013.
15. Li ZH, Hu PH, Tu JH and Yu NS: Luminal B breast cancer: Patterns of recurrence and clinical outcome. Oncotarget 7: 65024-65033, 2016.
16. Chun KH, Park JH and Fan S: Predicting and overcoming chemotherapeutic resistance in breast cancer. Adv Exp Med Biol 1026: 59-104, 2017.
17. Shiga K, Hara M, Nagasaki T, Sato T, Takahashi H and Takeyama H: Cancer-associated fibroblasts: Their characteristics and their roles in tumor growth. Cancers (Basel) 7: 2443-2458, 2015.
18. Barak V, Goike H, Panaretakis KW and Einarsson R: Clinical utility of cytokeratins as tumor markers. Clin Biochem 37: 529-540, 2004.
19. Xu-Monette ZY, Zhang M, Li J and Young KH: PD-1/PD-L1 blockade: Have we found the key to unleash the antitumor immune response? Front Immunol 8: 1597, 2017.
20. Jia L, Zhang Q and Zhang R: PD-1/PD-L1 pathway blockade works as an effective and practical therapy for cancer immunotherapy. Cancer Biol Med 15: 116-123, 2018.
21. Narayan P, Wahby S, Gao JJ, Amiri-Kordestani L, Ibrahim A, Bloomquist E, Tang S, Xu Y, Liu J, Fu W, *et al*: FDA approval summary: Atezolizumab plus paclitaxel protein-bound for the treatment of patients with advanced or metastatic TNBC whose tumors express PD-L1. Clin Cancer Res 26: 2284-2289, 2020.
22. Capp JP: Cancer stem cells: From historical roots to a new perspective. J Oncol 2019: 5189232, 2019.
23. Najafi M, Farhood B and Mortezaee K: Cancer stem cells (CSCs) in cancer progression and therapy. J Cell Physiol 234: 8381-8395, 2019.
24. Lathia JD and Liu H: Overview of cancer stem cells and stemness for community oncologists. Target Oncol 12: 387-399, 2017.
25. Visvader JE and Lindeman GJ: Cancer stem cells in solid tumours: Accumulating evidence and unresolved questions. Nat Rev Cancer 8: 755-768, 2008.

26. Sheridan C, Kishimoto H, Fuchs RK, Mehrotra S, Bhat-Nakshatri P, Turner CH, Goulet R Jr, Badve S and Nakshatri H: CD44$^{+}$/CD24$^{-}$ breast cancer cells exhibit enhanced invasive properties: An early step necessary for metastasis. Breast Cancer Res 8: R59, 2006.
27. Jonkman JE, Cathcart JA, Xu F, Bartolini ME, Amon JE, Stevens KM and Colarusso P: An introduction to the wound healing assay using live-cell microscopy. Cell Adh Migr 8: 440-451, 2014.
28. Meirson T and Gil-Henn H: Targeting invadopodia for blocking breast cancer metastasis. Drug Resist Updat 39: 1-17, 2018.
29. Gu W, Prasadam I, Yu M, Zhang F, Ling P, Xiao Y and Yu C: Gamma tocotrienol targets tyrosine phosphatase SHP2 in mammospheres resulting in cell death through RAS/ERK pathway. BMC Cancer 15: 609, 2015.
30. Dontu G, Al-Hajj M, Abdallah WM, Clarke MF and Wicha MS: Stem cells in normal breast development and breast cancer. Cell Prolif 36 (Suppl 1): S59-S72, 2003.
31. Bailey PC, Lee RM, Vitolo MI, Pratt SJP, Ory E, Chakrabarti K, Lee CJ, Thompson KN and Martin SS: Single-cell tracking of breast cancer cells enables prediction of sphere formation from early cell divisions. iScience 8: 29-39, 2018.
32. Bruner HC and Derksen PWB: Loss of E-cadherin-dependent cell-cell adhesion and the development and progression of cancer. Cold Spring Harb Perspect Biol 10: a029330, 2018.
33. Ziegler E, Hansen MT, Haase M, Emons G and Gründker C: Generation of MCF-7 cells with aggressive metastatic potential in vitro and in vivo. Breast Cancer Res Treat 148: 269-277, 2014.
34. Hazan RB, Phillips GR, Qiao RF, Norton L and Aaronson SA: Exogenous expression of N-cadherin in breast cancer cells induces cell migration, invasion, and metastasis. J Cell Biol 148: 779-790, 2000.
35. Huang H: Matrix metalloproteinase-9 (MMP-9) as a cancer biomarker and MMP-9 biosensors: Recent advances. Sensors (Basel) 18: 3249, 2018.
36. Li H, Qiu Z, Li F and Wang C: The relationship between MMP-2 and MMP-9 expression levels with breast cancer incidence and prognosis. Oncol Lett 14: 5865-5870, 2017.
37. Pivetta E, Scapolan M, Pecolo M, Wassermann B, Abu-Rumeileh I, Balestreri L, Borsatti E, Tripodo C, Colombatti A and Spessotto P: MMP-13 stimulates osteoclast differentiation and activation in tumour breast bone metastases. Breast Cancer Res 13: R105, 2011.
38. Weiswald LB, Bellet D and Dangles-Marie V: Spherical cancer models in tumor biology. Neoplasia 17: 1-15, 2015.
39. Rexer BN, Chanthaphaychith S, Dahlman KB and Arteaga CL: Direct inhibition of PI3K in combination with dual HER2 inhibitors is required for optimal antitumor activity in HER2+ breast cancer cells. Breast Cancer Res 16: R9, 2014.
40. Riaz M, van Jaarsveld MT, Hollestelle A, Prager-van der Smissen WJ, Heine AA, Boersma AW, Liu J, Helmijr J, Ozturk B, Smid M, *et al*: miRNA expression profiling of 51 human breast cancer cell lines reveals subtype and driver mutation-specific miRNAs. Breast Cancer Res 15: R33, 2013.
41. Hollestelle A, Nagel JH, Smid M, Lam S, Elstrodt F, Wasielewski M, Ng SS, French PJ, Peeters JK, Rozendaal MJ, *et al*: Distinct gene mutation profiles among luminal-type and basal-type breast cancer cell lines. Breast Cancer Res Treat 121: 53-64, 2010.
42. Chen CC, Feng W, Lim PX, Kass EM and Jasin M: Homology-directed repair and the role of BRCA1, BRCA2, and related proteins in genome integrity and cancer. Ann Rev Cancer Biol 2: 313-336, 2018.
43. Lord CJ and Ashworth A: Mechanisms of resistance to therapies targeting BRCA-mutant cancers. Nat Med 19: 1381-1388, 2013.
44. Moran A, O'hara C, Khan S, Shack L, Woodward E, Maher ER, Lalloo F and Evans DG: Risk of cancer other than breast or ovarian in individuals with BRCA1 and BRCA2 mutations. Fam Cancer 11: 235-242, 2012.
45. Ledermann JA, Drew Y and Kristeleit RS: Homologous recombination deficiency and ovarian cancer. Eur J Cancer 60: 49-58, 2016.
46. Gallagher DJ, Gaudet MM, Pal P, Kirchhoff T, Balistreri L, Vora K, Bhatia J, Stadler Z, Fine SW, Reuter V, *et al*: Germline BRCA mutations denote a clinicopathologic subset of prostate cancer. Clin Cancer Res 16: 2115-2121, 2010.
47. Iqbal J, Ragone A, Lubinski J, Lynch HT, Moller P, Ghadirian P, Foulkes WD, Armel S, Eisen A, Neuhausen SL, *et al*: The incidence of pancreatic cancer in BRCA1 and BRCA2 mutation carriers. Br J Cancer 107: 2005-2009, 2012.
48. Corcoran RB, Dias-Santagata D, Bergethon K, Iafrate AJ, Settleman J and Engelman JA: BRAF gene amplification can promote acquired resistance to MEK inhibitors in cancer cells harboring the BRAF V600E mutation. Sci Signal 3: ra84, 2010.
49. Kolinjivadi AM, Sannino V, de Antoni A, Técher H, Baldi G and Costanzo V: Moonlighting at replication forks-a new life for homologous recombination proteins BRCA1, BRCA2 and RAD51. FEBS Lett 591: 1083-1100, 2017.
50. Holloman WK: Unraveling the mechanism of BRCA2 in homologous recombination. Nat Struct Mol Biol 18: 748-754, 2011.
51. Shirole NH, Pal D, Kastenhuber ER, Senturk S, Boroda J, Pisterzi P, Miller M, Munoz G, Anderluh M, Ladanyi M, *et al*: TP53 exon-6 truncating mutations produce separation of function isoforms with pro-tumorigenic functions. Elife 5: e17929, 2016.
52. Shirole NH, Pal D, Kastenhuber ER, Senturk S, Boroda J, Pisterzi P, Miller M, Munoz G, Anderluh M, Ladanyi M, *et al*: TP53 exon-6 truncating mutations produce separation of function isoforms with pro-tumorigenic functions. Elife 6: e25532, 2017.
53. Huovinen M, Loikkanen J, Myllynen P and Vähäkangas KH: Characterization of human breast cancer cell lines for the studies on p53 in chemical carcinogenesis. Toxicol In Vitro 25: 1007-1017, 2011.
54. Hui L, Zheng Y, Yan Y, Bargonetti J and Foster D: Mutant p53 in MDA-MB-231 breast cancer cells is stabilized by elevated phospholipase D activity and contributes to survival signals generated by phospholipase D. Oncogene 25: 7305-7310, 2006.
55. Lu X, Errington J, Curtin NJ, Lunec J and Newell DR: The impact of p53 status on cellular sensitivity to antifolate drugs. Clin Cancer Res 7: 2114-2123, 2001.